ATLANTIS PRESS

Optimization of Chemical Activation Conditions for Activated Carbon From Coconut Shell Using Response Surface Methodology (RSM) and Its Ability to Adsorb CO₂

Nur Afiqah Anuwar[1*] Putri Faizura Megat Khamaruddin[1]

[1] *Faculty of Chemical Engineering, Universiti Teknologi MARA, 40450 Shah Alam, Selangor, Malaysia*
Email: afiqahanuwar1594@gmail.com

ABSTRACT

Coconut shell was used as a precursor to prepare activated carbon using potassium hydroxide (KOH) as a chemical activating agent for carbon dioxide (CO_2) adsorption at ambient conditions. The purpose of this study was to determine the optimum activation parameters of the activated carbon using Response Surface Methodology (RSM) to obtain high BET surface area. The factors and levels included were activation temperature (500-800 ℃), impregnation ratio of KOH (1-3) and activation time (32-120 min). The Brunauer-Emmett-Teller (BET) surface area was selected as the response. ANOVA analysis was used to identify the most influential factor in experimental design response. Scanning electron microscopy (SEM), infrared spectroscopy (FTIR) and low angle X-ray diffractometer (XRD) were used to further characterized the activated carbon prepared under the optimum range of activation conditions. The CO_2 adsorption of optimally prepared activated carbon at ambient conditions was observed. The optimum activation conditions for maximum porous development were; activation temperature 902. 27 ℃, impregnation ratio 3.68 and activation time 54.32 min. Under these conditions, the predicted BET surface area was 2083.61 m²/g. As the R^2 obtained from this model is 92.90%, it can be concluded that this model was reliable and the activated carbon from coconut shell impregnated with KOH is suitable for CO_2 adsorption process as it can generate high BET surface area.

Keywords: Adsorption, activated carbon, coconut shell, KOH activation, activation condition, Response Surface Methodology (RSM)

1. INTRODUCTION

Among all the adsorbents used in adsorption process for CO_2 removal, activated carbon seems to be a more promising alternative lately due to their variety of low cost precursors, good porosity network and easy to modify [1]. Defined as a carbonaceous materials that has high porosity by [2], the pore size of the activated carbon can be classified into; (i) micropores (<2nm), (ii) mesopores (between 2 and 50 nm), and (iii) macropores (>50 nm). The precursors for activated carbon can be both from synthetic (petroleum residues, coal and lignite) or naturally occurring (agricultural and biomass waste) carbonaceous solid raw materials. The selection of the raw material for the production of an activated carbon is a very important step as different type of precursors will produce a different quality, characteristics and properties of the produced activated carbon [2]. Recently, agricultural residues have been selected in many literatures as a precursor for the production of an activated carbon as they are highly available at cheap price.

Coconut shell as one of the agricultural waste had been widely used as a precursor in the production of activated carbon for various application due to its amorphous form of carbon that makes it a great adsorbent for gases, vapors and colloidal solids [3]. As it is also abundantly available around the world especially in Malaysia, it can lower the production cost of activated carbon, making it as a potential replacement of existing commercial adsorbents from non-renewable sources. In addition, activated carbon from coconut shells has an advantage of high density, high purity, and practically dust-free compared to other precursors [3]. It is also harder and more attrition-resistant [3]. Generally, according to [4], activated carbon produced from nut shells and stones are also known for their high surface area and well developed micropores structure.

There are two steps in the production of activated carbon. First, the carbonization step where the raw materials are carbonized in a furnace reactor at temperature below 800 ℃ in inert condition [4]. Second is the activation step where the carbonized product are required to undergo an activation process which is either physical or chemical treatment. Physical activation involves high temperature using either steam, carbon dioxide, air or their mixture as an oxidizing agents. While in chemical activation, the precursors are impregnated by an activating agents such as $ZnCl_2$, H_3PO_4, KOH and NaOH to help with the initial dehydration before being heated in inert condition.

Several factors influence the preparation of high-quality activated carbon. Activation temperature, impregnation ratio and activation time were the most influential factors

reported in the previous literatures [5][6][7]. It is particularly important to use an appropriate experimental design to optimize preparation conditions [8]. It has been found that Response Surface Methodology (RSM) is a useful tool for studying the interactions between two or more variables [9]. RSM's main advantage is the low number of experiments required to evaluate numerous parameters and their interactions [10]. A conventional way for optimizing a multi-factor process is to work with one variable at a time (OFAT), a time-consuming method that may not reveal the dynamic results and may circumvent optimum factor settings [8]. Optimization of experimental conditions using RSM has been widely applied in various processes including the preparation of activated carbons [11]. Some of the previous studies found in applying RSM in preparation of activated carbons were using precursors such as olive-waste cakes [12], Luscar char [13], Turkish lignite [9], rattan sawdust [14], coconut husk [15], flamboyant pods [16], oil palm fiber [17] and mangosteen peel [18].

The aim of this present work is to optimize the preparation conditions of an activated carbon from coconut shell using potassium hydroxide (KOH) activation to produce high BET surface area for CO_2 adsorption at ambient conditions. A central composite design (CCD) was selected to study simultaneously the effects of three numerical activated carbon preparation variables: activation temperature, impregnation ratio and activation time, on the BET surface area as a response. For its key porous properties, the activated carbon produced under the optimum range of conditions was characterized.

2. EXPERIMENTAL

2.1 Raw materials

The coconut shell is collected at Pasar Seksyen 16, Shah Alam from a local seller. Firstly, it is cleaned with distilled water to remove the dirt and impurities before dried in an oven at 110 ℃ for 24 hours to remove the surface moisture [19]. Then the dried coconut shell is powdered using grinder and ball mill and sieved to desired size range which is 63-125 µm [20].

2.2 Preparation of Activated Carbon

For carbonization process, the samples were loaded in a ceramic boat which was placed in a split tube furnace (OTF-1200X). The coconut shells were heated up to a carbonization temperature 700 ℃ at a heating rate of 10 ℃/min and were held for 2 hours at the carbonization temperatures under 200 mL/min nitrogen flow [21]. After carbonization, the samples were cooled to room temperature under the same nitrogen flow.

The samples were then impregnated with potassium hydroxide, (KOH) solution for chemical activation step using magnetic stirrer and hotplate at 60 ℃ for 2 hours. It then dried in an oven at 110 ℃ for 48 hours to eliminate any remaining moisture and then heated at the activation temperature under 10 ℃/min nitrogen flow in a split tube furnace (OTF-1200X). Lastly, it was washed with 1M HCl solution, followed by deionized water to remove any KOH residue from the material until the samples achieved pH 7-8 before being dried again in an oven for another 48 hours [22].

2.3 Experimental Design for Activated Carbon Preparation

Activation parameters for the preparation of activated carbon have been studied using a standard response surface methodology (RSM) design called a central composite design (CCD). This approach is ideal for fitting a quadratic surface and helps with a minimum number of experiments to optimize the effective parameters [22]. It can also be used to evaluate the parameter interaction [13]. The CCD is usually a 2n factorial run with 2n axial runs and n_c center runs (six replicates).

In this study, activated carbons were prepared through chemical activation process by using CCD to vary the preparation variables. Analyzed variables included activation temperature (A), impregnation ratio (B) and activation time (C). Based on literature and some preliminary studies, these three variables were selected along with their respective ranges.

A total of 23 complete factorial central composite designs were used for each categorical variable for the three variables, consisting of 8 factorial points, 6 axial points and 6 replicates at the center points, suggesting that a total of 20 experiments as calculated from equation (1) was needed [13]:

$$N = 2^n + 2n + n_c = 2^3 + (2)(3) + 6 = 20 \qquad (1)$$

where N is the total number of experiments required and n is the number of factors.

The center points were used to evaluate the experimental error and performance reproducibility. It includes six replications which are performed by setting all factors at their midpoints to estimate the residual error.

The independent variables are coded to the (−1, 1) interval where the low and high levels are coded as −1 and +1, respectively. The variables studied were activation temperature: 500-800 ℃, impregnation ratio: 1-3 and activation time: 32-120 min.

Table 1 shows the full design matrix of the experiments obtained. In order to limit the effects of uncontrolled factors, the experimental sequence was randomized.

Table 1 Experimental design matrix

No of Run	Factor A: Activation Temperature (°C)	Factor B: Impregnation Ratio	Factor C: Activation Time (min)
1	650.00	2.00	2.00
2	800.00	3.00	120.00
3	650.00	2.00	76.00
4	500.00	3.00	32.00
5	800.00	1.00	32.00
6	800.00	1.00	120.00
7	650.00	2.00	150.00
8	500.00	3.00	120.00
9	902.27	2.00	76.00
10	650.00	2.00	76.00
11	650.00	2.00	76.00
12	500.00	1.00	32.00
13	650.00	2.00	76.00
14	650.00	2.00	76.00
15	800.00	3.00	32.00
16	650.00	0.32	76.00
17	397.73	2.00	76.00
18	650.00	3.68	76.00
19	650.00	2.00	76.00
20	500.00	1.00	120.00

2.4 Response Variable Determination

The nitrogen adsorption/desorption isotherms will be measured at -196 °C using Micromeritics 3Flex Surface Analyzer. Prior to gas adsorption measurement, the samples will be degassed at 200 °C for 2 hours [23]. The specific surface area (S_{BET}) will be determined according to Brunauer-Emmett-Teller (BET) method.

2.5 Regression and Optimization Analysis

Minitab 18, a statistical analysis software was used to analyze experimental data for regression in order to fit the empirical mathematical model provided by equation (2) (24):

$$Y = b_0 + \sum_{i=1}^{n} b_i x_i + \left(\sum_{i=1}^{n} b_{ii} x_i \right)^2 + \sum_{i=1}^{n-1} \sum_{j=i+1}^{n} b_{ij} x_i x_j \tag{2}$$

where Y is the predicted response, b_0 the constant coefficient, b_i the linear coefficients, b_{ij} the interaction coefficients, b_{ii} the quadratic coefficients and x_i, x_j are the coded values of the activated carbon preparation variables. The following regression analysis, variance analysis (ANOVA) and contour plots were also analyzed using this tool. Models were used to generate response surface and contour plots to analyze the relationship between the experimental variables and the responses. R squared coefficient was used to estimate selected polynomial models' fitting quality. Optimum values are obtained from the optimizer. The importance and appropriateness of the system parameters were further investigated using the probability value (prob > F) and the F-value (Fisher Variation Ratio) [23]. For validation, once again, activated carbon will be produced under optimal conditions. The response will be measured. Also the predicted values of the correlations formed for each response were compared with the response values.

2.6 Characterization of Activated Carbon

The raw coconut shell, carbonized sample and optimally prepared activated carbon will be characterized by using analytical technique. The surface morphology will be observed using scanning electron microscopy, SEM (LEO 1450VP SEM).
The surface organic functional groups of samples were analyzed using FTIR spectroscopy (Pelkin Elmer Spectrum One). The IR spectrum was recorded from a wavenumber range of 500-4000 cm^{-1} [24].
Whereas, the crystalline structure were analyzed using low angle X-ray Diffractometer, XRD (PAN analytical, X'Pert-PRO) with Cu-Ka radiation (λ = 1.5406 Å) and diffraction angle (2Θ) from 5° to 80° [25].

2.7 CO2 Adsorption Measurement

Static CO_2 adsorption test of optimally prepared activated carbon was carried out using surface area and porosity analyzer (Micromeritics Tristar II Plus) at ambient temperature and pressure to observe its ability to adsorb CO_2 at ambient conditions. The pressure was varied from 0

to 1 bar while the temperature was at 25 ℃. The adsorbent degassing process was held at 150 ℃ for 24 hours.

3. RESULTS AND DISCUSSION

3.1. Response Surface Analysis

3.1.1 BET Surface Area of the Prepared Activated Carbons

Table 2 shows the full design matrix of the experiments along with the results obtained. The response considered in this study was BET surface area.

3.1.2 Pareto Chart

The Pareto chart shows the absolute values of the standardized effects from the greatest effect to the smallest effect. It is used to assess the magnitude and importance of the effects. The bars that cross the reference line on the Pareto chart are statistically significant. Since the Pareto graph only displays the absolute value of the effects, the magnitude of the effects can be determined (whether large or small), but it cannot be determined whether the effects will increase or decrease the response.

In the pareto chart in Figure 1, the relative importance of the main effects and their interactions are shown. The t-test was used to determine whether the effects measured differ significantly from zero [6]. The t-value was found to be equal to 2.228 for a confidence level of 95 percent and nine degrees of freedom. The horizontal column values are the t-test values for each effect [26][27][28]. Variable A, CC, B and BC have an absolute value greater than 2.228, which is placed on the right side of the vertical line and are important. Whereas all the other factors present an absolute value lower than the reference line which make them insignificant.

The figure also indicated that activation temperature (A), followed by two-way interactions (CC), activation ratio (B) and ratio-temperature interactions (BC), have the most important impact on the BET surface area of the activated carbon. The AC interactions have made the smallest contribution to the creation of BET surface area of activated carbon since it is very far away from the Pareto chart reference line.

3.1.3 Main Effects Plot

The main effect plot of the variables analyzed on the basis of the BET surface area is shown in Figure 2. The plot shows the mean deviations for each factor between the high and low levels.

By analyzing the results given in Figure 2, it can be concluded that the BET surface area of the activated carbon increase with the activation temperature. For impregnation ratio, BET surface area decrease when ratio increase from 0.31821 to 1 before increase with the increasing ratio afterwards. However for the activation time, the BET surface area of the activated carbon increases with activation time until 76 min before dropped with the prolong activation time.

Thermal degradation and the process of volatilization are further increased by the application of heat to impregnated material [3]. This results in pores being formed, surface area being increased and a subsequent mass loss. The temperature selection is based on several factors including the type of precursor and the chemical agent used. Temperatures vary between 400 and 800 °C for different biomass precursors [29]. In this study, BET surface area increases with the increase in activation temperature. This gradual temperature increase, increases the C-KOH reaction rate, resulting in an increase in "burn-off" carbon. At the same time, carbon sample volatility continues to evolve with an increase in activation temperature. Devolatization enhances the fundamental pore structure of the char while C-KOH reaction improves existing pores and produces new porosity [30]. These two reactions increase the BET surface area with an increase in activation temperature. The highest BET surface area 1555.39 m^2/g is achieved at 800 °C activation temperature. While at the maximum activation temperature which is 902.27 °C, BET surface area is 1527.28 m^2/g, which is

Table 2 Experimental result of the CCD design

No of Run	Factor A	Factor B	Factor C	BET Surface Area (m^2/g)
1	650.00	2.00	2.00	342.94
2	800.00	3.00	120.00	1119.78
3	650.00	2.00	76.00	785.54
4	500.00	3.00	32.00	596.25
5	800.00	1.00	32.00	825.60
6	800.00	1.00	120.00	1085.75
7	650.00	2.00	150.00	714.76
8	500.00	3.00	120.00	488.93
9	902.27	2.00	76.00	1527.28
10	650.00	2.00	76.00	1139.96
11	650.00	2.00	76.00	1033.68

12	500.00	1.00	32.00	420.18
13	650.00	2.00	76.00	1064.36
14	650.00	2.00	76.00	1083.98
15	800.00	3.00	32.00	1555.39
16	650.00	0.32	76.00	1002.58
17	397.73	2.00	76.00	377.44
18	650.00	3.68	76.00	1447.00
19	650.00	2.00	76.00	1092.27
20	500.00	1.00	120.00	505.40
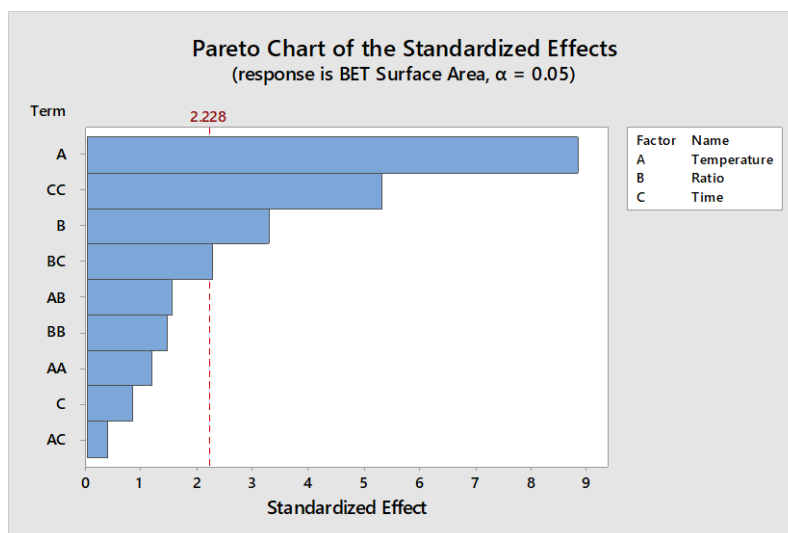
Figure 1 Pareto chart for BET surface area
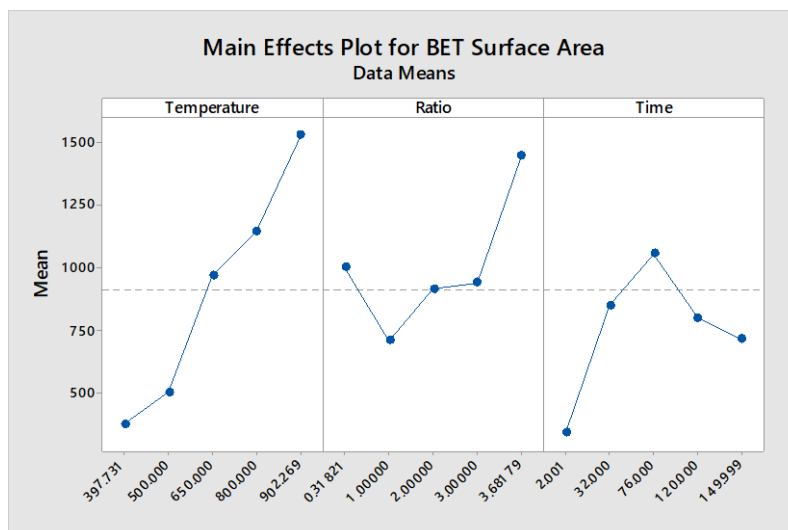
Figure 2 Main effects plot for BET surface area

the second highest reading. This is contradicted with the finding from [31], which indicated that a temperature increase does not always cause surface area development, and for most of the findings, a surface area decrease is observed on high temperatures, particularly in chemical activation where a surface area reduction is often observed at high temperatures between 450 and 800 °C. The different finding is obtained in this study might be a result of combination of highest activation temperature with medium impregnation ratio and low activation time. Although the sample undergoes highest activation temperature, it does not undergo prolong activation time

and high impregnation ratio. Furthermore, according to [8] the micropores are usually ruptured when the activation temperature exceeds 950 °C.

The impregnation ratio, the ratio of weights of the chemical agent and the dry precursor are well known to be one of the variables that has a major effect on the characteristics of the final carbon developed [3]. Thus, in addition to the effect on pores' development, especially the size, the resulting surface area is also affected by smaller pores that generally result in larger surface area. The general trend for all precursors is that the surface area also increases with increasing concentration. This is because the char interacts with KOH, forming K_2CO_3 with the parallel production of CO_2 and CO, thereby creating pores that will increase the surface area [32]. From result obtained in figure 2, low impregnation ratio between 0.32 and 1.00 produced low BET surface area, before it gradually increase with the increasing ratio. This is because impregnation ratio 0.32 is too low to speed up activation reaction rates and increase the number of pores. Moreover at this ratio, the activation temperature and time were also low which were 650 ℃ and 76 minutes respectively. The same trend can be seen happened to impregnation ratio 1.00. While [32] observed that a high KOH/char ratio could contribute to the accumulation of K_2CO_3 and metallic potassium that persisted in carbon and could not be easily removed even after repeated washing, which could contribute to the blockage of certain pores and a drastic reduction of the surface area, however in this study, although the impregnation ratio is high, the temperature and the time is low, resulting in high BET surface area as well. For example, at highest impregnation ratio 3.68, the activation temperature and time were 650 ℃ and 76 minutes respectively. This allows the activated carbon to develop pore perfectly.

With regard to the impact of the activation time, it is observed that the BET surface area of the activated carbon increases with increasing activation times until reaching a peak at the activation time 76 minutes, before it decreases with prolonged activation times. A longer carbonization time promoted reduction in BET surface area, presumably due to collapse of the smaller pores [33][34]. The activation time directly affects the creation of porous carbon networks. Time should be adequate to eliminate all moisture and volatile components of the precursor so that the pores can be formed [3]. Since the end of the volatile development marks the formation of the fundamental pore structure, activation should be limited to this stage. Longer periods lead to pore widening at surface area expense [3].

Variance analysis (ANOVA) has been used to further explain the model's adequacy [10]. Table 3 shows the results. This analysis is intended to investigate which factors have a significant impact on the activated carbon surface area. In this case, A (activation temperature), C^2 (activation time square), B (activation ratio) and BC (activation ratio*activation time) have a major influence on the activated carbon surface area, with P-value below level of significance, α=0.05. Values above 0.1000 indicate that the terms of the model are not significant. Consequently, the model that excluded were C (0.420), A^2 (0.261), B^2 (0.174), AB (0.152) and AC (0.702). However, the analysis shows that the model obtained to describe the process has a F-value of 14.53, which means that the model is significant [8]. The F-value for a model is the test to compare the variance associated with that term to the residual variance [10].

3.1.4 Statistical Analysis of the Result

Application of CCD for activated carbon production generated quadratic regression model for the BET surface area using Minitab 18 software as shown below;

BET Surface Area = -1742 + 3.91 Temperature – 225 Ratio + 22.80 Time – 0.00192 Temperature*Temperature + 53.1 Ratio*Ratio – 0.0997 Time*Time + 0.504 Temperature*Ratio – 0.00290 Temperature*Time – 2.52 Ratio*Time

The positive sign (+) in front of the terms indicates synergistic effect, while negative sign (-) indicates antagonistic effect [10].

The reliability of the developed model was evaluated on the basis of the correlation coefficient value. The coefficient of model correlation, R^2 was found to be 92.90%. R^2 value implies that 92.90% of the response variable variation is linked to the effect of the factors, so that 7.10% of the total variation is not explained by the model and is not predictable [8]. The R^2 value should be higher than 90.00% to show a good agreement between the models ' experimental and projected values [10]. If they aren't, either the data or the model may have a problem [10].

**Table 3** Analysis of variance for BET surface area

Source	DF	Adj SS	Adj MS	F-Value	P-Value	
Model	9	2480525	275614	14.53	0.000	
Linear	3	1706890	568963	30.00	0.000	
Temperature	1	1489071	1489071	78.52	0.000	Significant
Ratio	1	204421	204421	10.78	0.008	Significant
Time	1	13398	13398	0.71	0.420	
Square	3	626428	208809	11.01	0.002	
Temperature*Temperature	1	26964	26964	1.42	0.261	

Ratio*Ratio	1	40578	40578	2.14	0.174	
Time*Time	1	536746	536746	28.30	0.000	Significant
2-Way Interaction	3	147207	49069	2.59	0.111	
Temperature*Ratio	1	45635	45635	2.41	0.152	
Temperature*Time	1	2940	2940	0.16	0.702	
Ratio*Time	1	98632	98632	5.20	0.046	Significant
Error	10	189636	18964			
Lack-of-Fit	5	109864	21973	1.38	0.367	
Pure Error	5	79771	15954			
Total	19	2670161				

3.1.5 Contour Plot
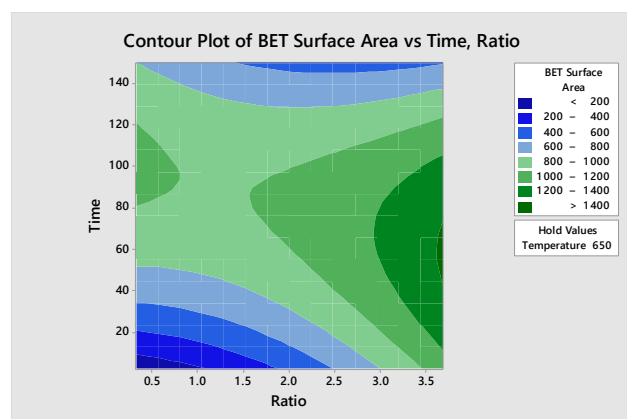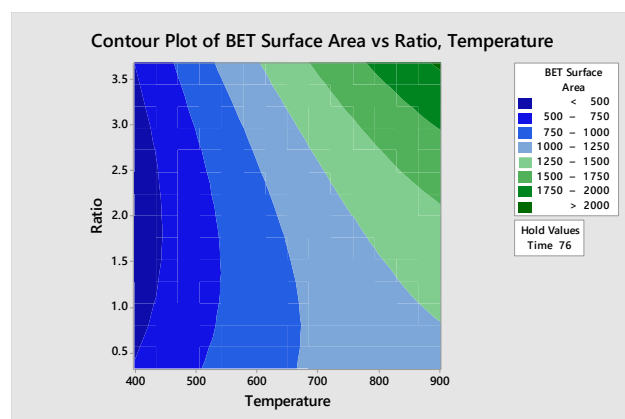
(a) (b)

Figure 3 Contour plot for BET surface area (a) Time vs Ratio and (b) Temperature vs Ratio

The contour diagram of the most significant factors BC (activation ratio and activation time) and AB (activation temperature and activation ratio) are illustrated in Figure 3 to better explain the impact of factors on the activation process. The contour plot of the response surface is shown when one parameter is at a hold value. The contour plots are curved lines due to the factors interactions in the model. The optimum conditions can be found within the region of the highest BET surface area.

From Figure 3 (a), the activation temperature was hold at 650 ℃. At low impregnation ratio 0.5 to 3.0 and shorter activation time 20 to 50 minutes, low BET surface area was observed. However, at low impregnation ratio but longer activation time from 55 to 150 minutes, the BET surface area gradually increased. High impregnation ratio from 3.0 to >3.5 together with longer activation time produced highest BET surface area but it can also be observed that if at highest impregnation ratio and longer activation time more than 150 minutes, the BET surface area will significantly decrease.

The relationship between impregnation ratio and activation temperature can be seen from Figure 3 (b). It can be observed that at high activation temperature from 620 ℃ to 900 ℃ and high impregnation ratio from 0.8 to 3.5, the BET surface area gradually increasing. The highest BET surface area was produced at the highest activation temperature and impregnation ratio. The hold value of activation time was 76 minutes.
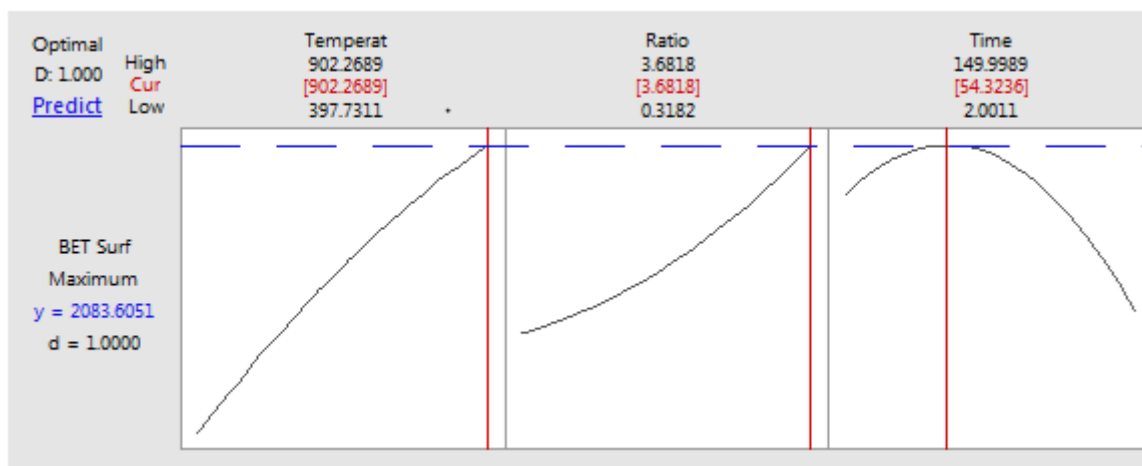
Figure 4 Optimization plot

From optimization plot (Figure 4) calculated by Minitab 18, the overall optimum impregnation ratio is 3.68 while the ideal impregnation ratio range obtained from the contour plot AB is between 2.2 - 3.68. Although in previous studies [34][29] stated that the high ratios will lead to the reduction of surface area in activated carbon, this phenomena was not happen in this present study. It might because although high impregnation ratio was applied, the sample was only undergoes low activation temperature and short activation time, resulting in well-developed porosity.

The optimum range for the activation time was between 44 to 68 min, while the optimum point obtained from Minitab 18 optimization plot was 54.32 min. Owing to the reduction of volatiles and eventual rearrangement of the remaining structures, the optimum activation time found to enable pore creation was adequate [3]. The defined range suggested that activation does not need to be extended so far beyond the basic requirement, as this would cause pores to be enlarged [3]. In addition, longer duration naturally often implies greater energy costs, as the elevated activation temperature needs to be sustained for a longer time. As for the activation temperature, the overall optimum temperature obtained from Minitab 18 optimization plot is 902.27 °C while the ideal temperature range obtained from the contour plot is 700-902.27 °C. The optimum temperature range was found equal to 394-416 °C in a previous study on coconut shell chemical activation using phosphoric acid [3]. This range is smaller than this study's temperature range. The optimum temperature range found by [3] however, was based on multiple responses, not only on one response (BET surface area) as in this work.

3.2 Process Optimization

One of the main objective in this study is to find the optimum activation parameters at which activated carbon will have high BET surface area to enhance CO_2 adsorption at ambient conditions. The optimum values of the preparation conditions were calculated from the optimizer model in Minitab 18. In this optimization analysis, the activation parameters (activation temperature, impregnation ratio and activation time) were selected to be "within the range' while the response (BET surface area) was set as "maximum". Activated carbon were then prepared under the optimum conditions given in Table 4, together with the predicted and experimental value for BET surface area.

Table 4 shows that the experimental value obtained for BET surface area is in good agreement with the value predicted from the model. The error percentage (%) between the predicted and the actual value shows relatively small value which is below 10%, indicating the accuracy of the optimization process [35].

Table 5 lists the comparison of maximum BET surface area on various activated carbon. The activated carbon prepared in this work is one of the study that had a relatively high BET surface area compared to some other adsorbents reported in the literatures. This suggested that the preparation method and operating conditions used in this study should be used for the processing of activated carbon from coconut shell with high BET surface area for CO2 adsorption.

Table 4 Process optimization results

Optimum preparation conditions			BET surface area (m²/g)		
Activation temperature (℃)	Impregnation ratio	Activation time (min)	Predicted	Experimental	Error
902.27	3.68	54.32	2083.61	2157.98	3.60

Table 5 Comparison of maximum BET surface area on various activated carbon

Adsorbent	Maximum BET surface area (m^2/g)	Reference
Coconut shell based activated carbon	2157.98	This work
Olive cake based activated carbon	672.70	(6)
Textile sewage sludge (TSS) based activated carbon	336.14	(10)
Olive tree pruning (OTP) based activated carbon	3514.25	(8)
Rice husk based activated carbon	2700.00	(38)

3.3 Characterization of Raw, Carbonized and Optimally Prepared Activated Carbon

3.3.1 Surface Morphology

SEM analysis was conducted to observe the surface morphology of the samples. From Figure 5, results showed after carbonization at 700 ℃, pore developed on the surface of the sample become smaller compared to the pore developed in the raw sample. This is due to the purpose of carbonization process which is to enrich the carbon content and create initial porosity in the chars [36]. At high carbonization temperature, great amount of volatiles were released from the raw coconut shell and eventually developed micropore [37]. However small material debris can be seen on the surface of the carbonized samples, which can prohibit the adsorbate transfer to the carbon cores [38]. SEM image of optimally prepared activated carbon with optimum activation parameters (activation temperature 902.27 ℃, impregnation ratio 3.68 and activation time 54.32 min) was shown is Figure 5 (c). As expected, impregnation with KOH produced a smooth surface of activated carbon [39] with numerous micropores opening and well-develop porosity compared to the raw and carbonized carbon samples [40]. The existence of perfect pores is dominant, uniform in size and distributed randomly on the activated carbon surface. The pores are perfectly structured with clear openings which allow access to internal pores. The surface is clean with no clogging pores ready for adsorption. This may be due to a washing procedure after heat treatment during activation [38].

3.3.2 Surface Chemistry

Figure 6, shows the FTIR spectra for raw coconut shell with particle size 63-125 μm, carbonized sample with the same particle size and carbonization temperature of 700 ℃ and optimally prepared activated carbon. The adsorbent FTIR spectrum is essential for identifying the active functional groups on the surface of raw material the adsorbent. In general, we can see from the IR spectrum, that all peaks produce weak transmittance. This shows that either untreated or activated carbon sample have very little and poor concentrations of functional groups [38]. In addition all samples show remarkably identical spectra, indicating similar structure and functional groups. However, spectra intensity varies slightly from the raw coconut shell to the activated carbon.
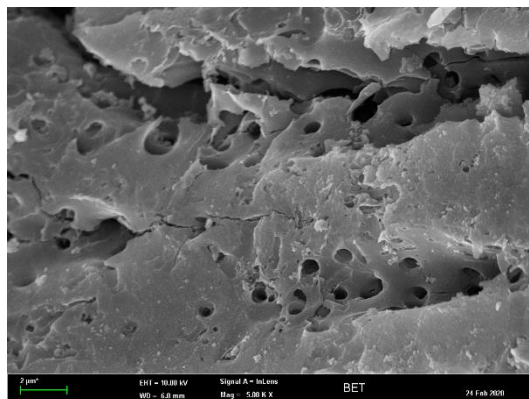
As stated in many earlier studies [41][42], numerous functional groups were present on the raw materials. The spectrum indicates the existence of certain common bands of coconut shell lignocellulosic materials belonging to functional groups, such as hydroxyl, alkenes,
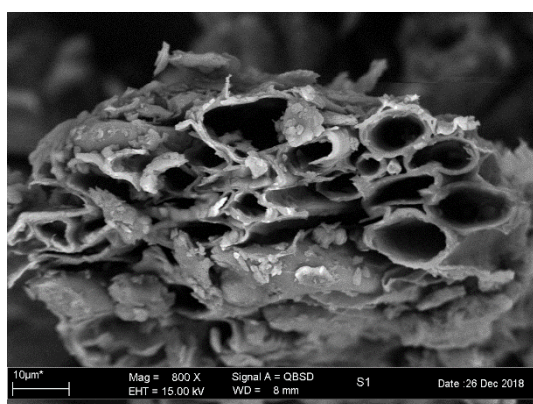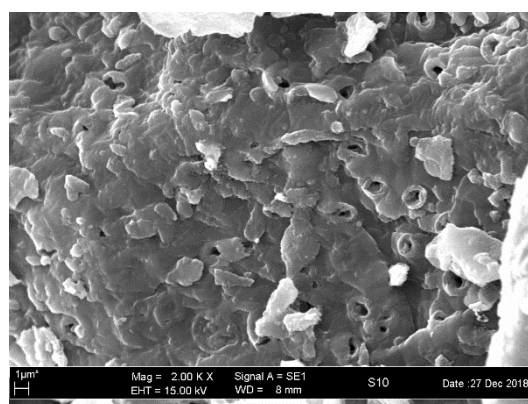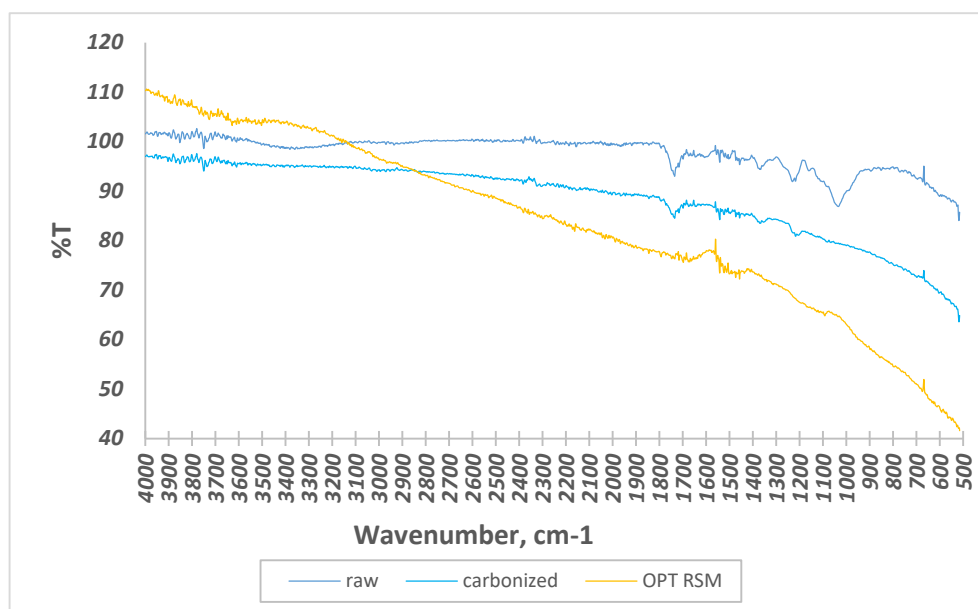

(a)   (b)

(c)

Figure 5 SEM images of (a) raw sample with particle size 63-125 μm (b) carbonized carbon samples with particle size 63-125 μm, carbonization temperature of 700 ℃ and (c) optimally prepared activated carbon

Figure 6 Fourier-transform infrared spectroscopy (FTIR) spectra of raw (63-125 μm), carbonized (63-125 μm, 700 ℃) and optimally prepared activated carbon sample

aromatics, and carbonyls [43]. O-H stretching vibration in protein, cellulose, hemicellulose, lignin structure or absorbed water is attributed to the broad peak at 3550 cm^{-1} to 3200 cm^{-1} [44][45]. The bands at 1460 cm^{-1}, 1390 cm^{-1}, 1300 cm^{-1} and 1220 cm^{-1} is indicative of a scissor vibration of methylene, aldehydes, C-O stretching in cellulose and =C-O-C anti-symmetric vibrations connected to lignin aromatic rings, respectively [49]. In addition, the C-O bonds in ethers or polysaccharides corresponding to the peak at 1020 cm^{-1} are often stated in terms of cellulose [50]. A series of peaks ranging from 1600 cm^{-1} and 1470 cm^{-1} were considered coconut lignin aromatic skeleton vibrations. Absorption peaks in raw coconut shell corresponding to carbonaceous organics significantly decreased in the carbonized sample, particularly in the ranges 3550 cm^{-1} to

3200 cm^{-1}. The peak is associated with hydroxyl decreased significantly, indicating hydroxyl dehydration or evaporation of absorbed water. Carbonized spectrum is closely identical to optimally prepared activate carbon but with smoothened curve. Optimally prepared activated carbon exhibits O–H stretching vibration band of hydroxyl group at wavelength 3550 cm^{-1}. No formation of hydroxyl group is observed in carbonized sample thus suggesting that the formation is only took place after the char is activated [46]. Peak improvement at about 1500 cm^{-1} from carbonized sample to optimally prepared carbon sample can be a sign of aromatization of carbon due to the heat treatment during activation [38]. Presence of alkyne and aromatics can be observed through C C triple bond and C=C stretching vibrations, respectively at wavelengths 2310

cm^{-1} and 1560 cm^{-1}. The similar peaks are also observed in carbonized sample but with lesser intensities. Vibrations between 1700 cm^{-1} and 1550 cm^{-1} could be assigned to alkenes conjugation (C=C) as one of the characteristics of cellulose and hemicelluloses [47]. The band at 1200 and 1100 cm^{-1} could be a result of C-O stretching vibrations in tertiary, secondary and primary alcohol that is more evident

in the carbonized sample [48]. The FTIR result shows that all the samples activated carbons are rich in basic surface functional group which in turn helps in the CO_2 adsorption process [49].

3.3.3 *X-ray Diffraction (XRD) Analysis*

(a)

(b)
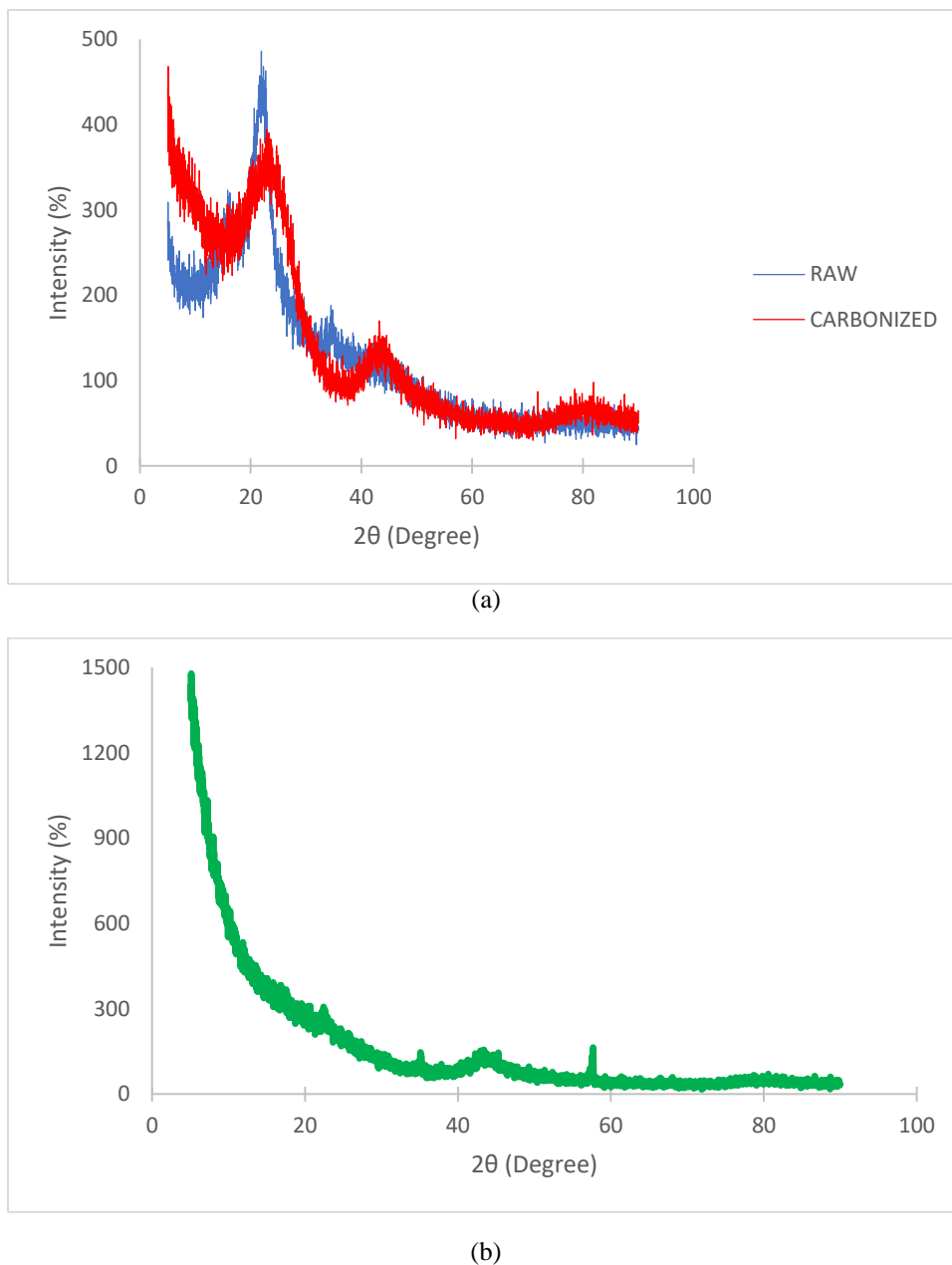
Figure 7 XRD pattern for (a) raw and carbonized samples, (b) optimally prepared activated carbon

The XRD pattern for raw, carbonized and optimally prepared activated carbon from coconut shell impregnated with KOH are shown in figure 7. From these figure, it can be observed that all the samples exhibit two broad

diffraction peaks located at 2θ = 20°-35° and 40°-50°. It revealed the presence of amorphous structure which is disorderly stacked up by carbon rings and helpful for producing well defined adsorbent [50][40][39]. This finding

also suggests that all the samples have poor crystallinity making it a good adsorbent as higher crystallinity will lower the porosity and hence the surface area, and should lead to a "cleaner" surface, with less moieties and less defects, which are known to be energetic sites that are preferentially used for adsorption [21].

3.4 Static CO_2 Adsorption at Ambient Conditions

Optimally prepared activated carbon was send to undergo static CO_2 adsorption at ambient conditions. From the results, it shows that optimally prepared activated carbon from coconut shell impregnated with KOH can adsorbed quite a promising number of CO_2 at ambient conditions which was 3.3144 mmol/g. This value is comparable to some known adsorbents at same temperature (25 ℃) and pressure (1 bar); starch and cellulose derived porous carbon showed 3.50 mmol/g CO_2 uptake [51], porous nitrogen-doped carbon synthesized by carbonization of coconut shell followed by urea modification and K_2CO_3 activation showed CO_2 capture capacity of 3.71 mmol/g [20], nitrogen-doped porous carbons using polypyrrole as the precursor obtained a CO_2 adsorption capacity of 3.9 mmol/g [52], and MOF-177 has CO_2 adsorption capacity of 0.999 mmol/g [53].

4. CONCLUSION

The present research revealed that coconut shell is a potential precursor for preparation of highly porous activated carbon by KOH activation for CO_2 adsorption at ambient conditions. Response Surface Methodology (RSM) was used to optimize the effects of activation temperature, impregnation ratio and activation time on BET surface area. The model's validity was effectively confirmed by experimental data. Process optimization was performed and the experimental value for the BET surface was found to be satisfactory with the one predicted. The optimum activation parameters to obtain maximum BET surface area 2083.61 m^2/g were; activation temperature 902. 27 ℃, impregnation ratio 3.68 and activation time 54.32 min. From experiment, the BET surface area obtained by preparing the activated carbon based on those parameters was 2157.98 m^2/g. Pareto chart indicated that activation temperature (A) has the most significant effect on the BET surface area of the activated carbon, followed by two way interactions (CC), activation ratio (B) and ratio-temperature interactions (BC). In addition, CO_2 adsorption capacity of the optimally prepared activated carbon showed promising result. However, in order to enhance the CO_2 adsorption application using this activated carbon, more thorough works need to be done to study the effects of activation parameters on the CO_2 adsorbed at ambient temperature and also the relationship between BET surface area and CO_2 adsorption capacity of activated carbon. Thus, it is concluded from the study that activated carbon from coconut shell impregnated with KOH

is a potential adsorbents that can produce high BET surface area for CO_2 adsorption process.

ACKNOWLEDGMENT

REFERENCES

[1] N. A. Rashidi and S. Yusup, "An overview of activated carbons utilization for the post-combustion carbon dioxide capture," *Biochem. Pharmacol.*, vol. 13, pp. 1–16, 2016, doi: 10.1016/j.jcou.2015.11.002.

[2] M. A. Yahya, Z. Al-Qodah, and C. W. Z. Ngah, "Agricultural bio-waste materials as potential sustainable precursors used for activated carbon production: A review," *Renew. Sustain. Energy Rev.*, vol. 46, pp. 218–235, 2015, doi: 10.1016/j.rser.2015.02.051.

[3] M. K. B. Gratuito, T. Panyathanmaporn, and R. Chumnanklang, "Production of activated carbon from coconut shell : Optimization using response surface methodology," vol. 99, pp. 4887–4895, 2008, doi: 10.1016/j.biortech.2007.09.042.

[4] O. Ioannidou and A. Zabaniotou, "Agricultural residues as precursors for activated carbon production-A review," *Renew. Sustain. Energy Rev.*, vol. 11, no. 9, pp. 1966–2005, 2007, doi: 10.1016/j.rser.2006.03.013.

[5] J. M. Salman, "Optimization Study of Pesticides Removal by Olives Trees Stalks Activated Carbon Using Response Surface Methodology," no. November, 2015.

[6] N. T. Abdel-ghani, G. A. El-chaghaby, M. H. Elgammal, and E. A. Rawash, "Optimizing the preparation conditions of activated carbons from olive cake using KOH activation," *New Carbon Mater.*, vol. 31, no. 5, pp. 492–500, 2016, doi: 10.1016/S1872-5805(16)60027-6.

[7] H. S. Niasar, H. Li, S. Das, T. V. R. Kasanneni, M. B. Ray, and C. (Charles) Xu, "Preparation of activated petroleum coke for removal of naphthenic acids model compounds: Box-Behnken design optimization of KOH activation process," *J. Environ. Manage.*, vol. 211, pp. 63–72, 2018, doi: 10.1016/j.jenvman.2018.01.051.

[8] A. Mamaní, M. F. Sardella, M. Giménez, and C. Deiana, "Highly microporous carbons from olive tree pruning: Optimization of chemical activation conditions," *J. Environ. Chem. Eng.*, vol. 7, no. 1, p. 102830, 2019, doi: 10.1016/j.jece.2018.102830.

[9] F. Karacan and U. Ozden, "Optimization of manufacturing conditions for activated carbon from Turkish lignite by chemical activation using response surface methodology," vol. 27, pp. 1212–1218, 2007, doi: 10.1016/j.applthermaleng.2006.02.046.

[10] E. Kacan, "Optimum BET surface areas for activated carbon produced from textile sewage sludges and its application as dye removal," *J. Environ. Manage.*, vol. 166, pp. 116–123, 2016, doi: 10.1016/j.jenvman.2015.09.044.

[11] H. El Bakouri, J. Morillo, J. Usero, and A. Ouassini, "Natural attenuation of pesticide water contamination by using ecological adsorbents: Application for chlorinated pesticides included in European Water Framework Directive," *J. Hydrol.*, vol. 364, no. 1–2, pp. 175–181, 2009, doi: 10.1016/j.jhydrol.2008.10.012.

[12] A. Baçaoui *et al.*, "Optimization of conditions for the preparation of activated carbons from olive-waste cakes," *Carbon N. Y.*, vol. 39, no. 3, pp. 425–432, 2001, doi: 10.1016/S0008-6223(00)00135-4.

[13] R. Azargohar and A. K. Dalai, "Production of activated carbon from Luscar char: Experimental and modeling studies," *Microporous Mesoporous Mater.*, vol. 85, no. 3, pp. 219–225, 2005, doi: 10.1016/j.micromeso.2005.06.018.

[14] A. A. Ahmad, B. H. Hameed, and A. L. Ahmad, "Removal of disperse dye from aqueous solution using waste-derived activated carbon: Optimization study," *J. Hazard. Mater.*, 2009, doi: 10.1016/j.jhazmat.2009.05.021.

[15] I. A. W. Tan, A. L. Ahmad, and B. H. Hameed, "Optimization of preparation conditions for activated carbons from coconut husk using response surface methodology," *Chem. Eng. J.*, vol. 137, no. 3, pp. 462–470, 2008, doi: 10.1016/j.cej.2007.04.031.

[16] A. M. M. Vargas, C. A. Garcia, E. M. Reis, E. Lenzi, W. F. Costa, and V. C. Almeida, "NaOH-activated carbon from flamboyant (Delonix regia) pods: Optimization of preparation conditions using central composite rotatable design," *Chem. Eng. J.*, vol. 162, no. 1, pp. 43–

50, 2010, doi: 10.1016/j.cej.2010.04.052.

[17] B. H. Hameed, I. A. W. Tan, and A. L. Ahmad, "Optimization of basic dye removal by oil palm fibre-based activated carbon using response surface methodology," *J. Hazard. Mater.*, 2008, doi: 10.1016/j.jhazmat.2008.01.088.

[18] M. A. Ahmad and R. Alrozi, "Optimization of preparation conditions for mangosteen peel-based activated carbons for the removal of Remazol Brilliant Blue R using response surface methodology," *Chem. Eng. J.*, 2010, doi: 10.1016/j.cej.2010.10.049.

[19] A. S. Ello, L. K. C. De Souza, A. Trokourey, and M. Jaroniec, "Development of microporous carbons for CO2capture by KOH activation of African palm shells," *J. CO2 Util.*, vol. 2, pp. 35–38, 2013, doi: 10.1016/j.jcou.2013.07.003.

[20] J. Chen *et al.*, "Enhanced CO2Capture Capacity of Nitrogen-Doped Biomass-Derived Porous Carbons," *ACS Sustain. Chem. Eng.*, vol. 4, no. 3, pp. 1439–1445, 2016, doi: 10.1021/acssuschemeng.5b01425.

[21] W. Li, K. Yang, J. Peng, L. Zhang, S. Guo, and H. Xia, "Effects of carbonization temperatures on characteristics of porosity in coconut shell chars and activated carbons derived from carbonized coconut shell chars," *Ind. Crops Prod.*, vol. 28, no. 2, pp. 190–198, 2008, doi: 10.1016/j.indcrop.2008.02.012.

[22] J. M. Salman, "Optimization of preparation conditions for activated carbon from palm oil fronds using response surface methodology on removal of pesticides from aqueous solution," *Arab. J. Chem.*, vol. 7, no. 1, pp. 101–108, 2014, doi: 10.1016/j.arabjc.2013.05.033.

[23] Z. N. Garba and A. A. Rahim, "Process optimization of K 2 C 2 O 4 -activated carbon from Prosopis africana seed hulls using response surface methodology," *J. Anal. Appl. Pyrolysis*, 2014, doi: 10.1016/j.jaap.2014.03.016.

[24] A. K. Thakur, R. Bilash, M. Majumder, and G. Gupta, "Electrochimica Acta In-Situ Integration of Waste Coconut Shell Derived Activated Carbon / Polypyrrole / Rare Earth Metal Oxide (Eu 2 O 3): A Novel Step Towards Ultrahigh Volumetric Capacitance," *Electrochim. Acta*, vol. 251, pp. 532–545, 2017, doi: 10.1016/j.electacta.2017.08.159.

[25] A. R. Hidayu and N. Muda, "Preparation and Characterization of Impregnated Activated

Carbon from Palm Kernel Shell and Coconut Shell for CO2 Capture," *Procedia Eng.*, vol. 148, pp. 106–113, 2016, doi: 10.1016/j.proeng.2016.06.463.

[26] S. Saadat and A. Karimi-Jashni, "Optimization of Pb(II) adsorption onto modified walnut shells using factorial design and simplex methodologies," *Chem. Eng. J.*, vol. 173, no. 3, pp. 743–749, 2011, doi: 10.1016/j.cej.2011.08.042.

[27] A. Rathinam, J. R. Rao, and B. U. Nair, "Adsorption of phenol onto activated carbon from seaweed: Determination of the optimal experimental parameters using factorial design," *J. Taiwan Inst. Chem. Eng.*, vol. 42, no. 6, pp. 952–956, 2011, doi: 10.1016/j.jtice.2011.04.003.

[28] M. E. R. Carmona, M. A. P. Da Silva, and S. G. Ferreira Leite, "Biosorption of chromium using factorial experimental design," *Process Biochem.*, vol. 40, no. 2, pp. 779–788, 2005, doi: 10.1016/j.procbio.2004.02.024.

[29] Y. Diao, W. P. Walawender, and L. T. Fan, "Activated carbons prepared from phosphoric acid activation of grain sorghum," vol. 81, pp. 2–9, 2002.

[30] A. C. Lua and T. Yang, "Effect of activation temperature on the textural and chemical properties of potassium hydroxide activated carbon prepared from pistachio-nut shell," *J. Colloid Interface Sci.*, vol. 274, no. 2, pp. 594–601, 2004, doi: 10.1016/j.jcis.2003.10.001.

[31] T. Alslaibi, I. Abustan, M. Ahmad, and A. A. Foul, "Review: Comparison of agricultural by-products activated carbon production methods using surface area response," *Cjasr*, no. August, pp. 528–538, 2013, [Online]. Available: http://scholar.google.com/scholar?hl=en&btnG=Search&q=intitle:Review+:+Comparison+of+agricultural+by-products+activated+carbon+production+methods+using+surface+area+response+Activation+processes#0.

[32] I. A. W. Tan, A. L. Ahmad, and B. H. Hameed, "Preparation of activated carbon from coconut husk: Optimization study on removal of 2,4,6-trichlorophenol using response surface methodology," *J. Hazard. Mater.*, vol. 153, no. 1–2, pp. 709–717, 2008, doi: 10.1016/j.jhazmat.2007.09.014.

[33] C. Srinivasakannan, M. Zailani, and A. Bakar, "Production of activated carbon from rubber wood sawdust," vol. 27, pp. 89–96, 2004, doi: 10.1016/j.biombioe.2003.11.002.

[34] T. Vernersson, P. R. Bonelli, E. G. Cerrella, and A. L. Cukierman, "Arundo donax cane as a precursor for activated carbons preparation by phosphoric acid activation," vol. 83, pp. 95–104, 2002.

[35] T. Mahmood, R. Ali, A. Naeem, M. Hamayun, and M. Aslam, "Potential of used Camellia sinensis leaves as precursor for activated carbon preparation by chemical activation with H3PO4; optimization using response surface methodology," *Process Saf. Environ. Prot.*, vol. 109, pp. 548–563, 2017, doi: 10.1016/j.psep.2017.04.024.

[36] W. Li, K. Yang, J. Peng, L. Zhang, S. Guo, and H. Xia, "Effects of carbonization temperatures on characteristics of porosity in coconut shell chars and activated carbons derived from carbonized coconut shell chars," vol. 8, pp. 190–198, 2008, doi: 10.1016/j.indcrop.2008.02.012.

[37] W. Mohd, A. Wan, W. Shabuddin, W. Ali, and M. Z. Sulaiman, "The effects of carbonization temperature on pore development in palm-shell-based activated carbon," vol. 0008, pp. 1925–1932, 2000.

[38] C. W. Purnomo, E. P. Kesuma, I. Perdana, and M. Aziz, "Lithium recovery from spent Li-ion batteries using coconut shell activated carbon," *Waste Manag.*, vol. 79, pp. 454–461, 2018, doi: 10.1016/j.wasman.2018.08.017.

[39] H. Demiral, "Pore structure of activated carbon prepared from hazelnut bagasse by chemical activation Pore structure of activated carbon prepared from hazelnut bagasse by chemical activation," no. MARCH 2008, 2016, doi: 10.1002/sia.2631.

[40] T. Kawano, M. Kubota, and M. S. Onyango, "Preparation of activated carbon from petroleum coke by KOH chemical activation for adsorption heat pump," vol. 28, pp. 865–871, 2008, doi: 10.1016/j.applthermaleng.2007.07.009.

[41] A. Islam, M. J. Ahmed, W. A. Khanday, M. Asif, and B. H. Hameed, "Mesoporous activated coconut shell-derived hydrochar prepared via hydrothermal carbonization-NaOH activation for methylene blue adsorption," *J. Environ. Manage.*, vol. 203, pp. 237–244, 2017, doi: 10.1016/j.jenvman.2017.07.029.

[42] W. H. Li *et al.*, "Preparation of sludge-based activated carbon made from paper mill sewage sludge by steam activation for dye wastewater treatment," *Desalination*, vol. 278, no. 1–3, pp. 179–185, 2011, doi: 10.1016/j.desal.2011.05.020.

[43] J. Mohammed, N. S. Nasri, M. A. Ahmad Zaini, U. D. Hamza, and F. N. Ani, "Adsorption of benzene and toluene onto KOH activated coconut shell based carbon treated with NH3," *Int. Biodeterior. Biodegrad.*, vol. 102, pp. 245–255, 2015, doi: 10.1016/j.ibiod.2015.02.012.

[44] M. J. Prauchner and F. Rodríguez-Reinoso, "Chemical versus physical activation of coconut shell: A comparative study," *Microporous Mesoporous Mater.*, vol. 152, no. January 2016, pp. 163–171, 2012, doi: 10.1016/j.micromeso.2011.11.040.

[45] J. Wang, T. L. Liu, Q. X. Huang, Z. Y. Ma, Y. Chi, and J. H. Yan, "Production and characterization of high quality activated carbon from oily sludge," *Fuel Process. Technol.*, vol. 162, pp. 13–19, 2017, doi: 10.1016/j.fuproc.2017.03.017.

[46] A. T. M. Din, B. H. Hameed, and A. L. Ahmad, "Batch adsorption of phenol onto physiochemical-activated coconut shell," vol. 161, pp. 1522–1529, 2009, doi: 10.1016/j.jhazmat.2008.05.009.

[47] Y. Sun and P. A. Webley, "Preparation of activated carbons from corncob with large specific surface area by a variety of chemical activators and their application in gas storage," *Chem. Eng. J.*, vol. 162, no. 3, pp. 883–892, 2010, doi: 10.1016/j.cej.2010.06.031.

[48] J. M. V. Nabais, C. E. C. Laginhas, P. J. M. Carrott, and M. M. L. Ribeiro Carrott, "Production of activated carbons from almond shell," *Fuel Process. Technol.*, vol. 92, no. 2, pp. 234–240, 2011, doi: 10.1016/j.fuproc.2010.03.024.

[49] J. Mohammed, N. Shawal, M. Abbas, A. Zaini, U. Dadum, and F. Nasir, "International Biodeterioration & Biodegradation Adsorption of benzene and toluene onto KOH activated coconut shell based carbon treated with NH 3," *Int. Biodeterior. Biodegradation*, vol. 102, pp. 245–255, 2015, doi: 10.1016/j.ibiod.2015.02.012.

[50] L. A. M. Rocha, K. A. Andreassen, and C. A. Grande, "Separation of CO 2 / CH 4 using carbon molecular sieve (CMS) at low and high pressure," *Chem. Eng. Sci.*, vol. 164, pp. 148–157, 2017, doi: 10.1016/j.ces.2017.01.071.

[51] M. Sevilla and A. B. Fuertes, "Sustainable porous carbons with a superior performance for CO2 capture," *Energy Environ. Sci.*, vol. 4, no. 5, pp. 1765–1771, 2011, doi: 10.1039/c0ee00784f.

[52] M. Sevilla, P. Valle-vigón, A. B. Fuertes, I. Nacional, and P. O. Box, "N-doped polypyrrole-based porous carbons for CO 2 capture **."

[53] S. Ullah *et al.*, "Synthesis, and characterization of metal-organic frameworks -177 for static and dynamic adsorption behavior of CO2 and CH4," *Microporous Mesoporous Mater.*, vol. 288, no. June, p. 109569, 2019, doi: 10.1016/j.micromeso.2019.109569.